Egyptian Geophysical Society
EGS Journal, Vol. 13, No. 1, 21-34 (2015)

THIN BED EVALUATION USING NUCLEAR MAGNETIC RESONANCE DATA INTEGRATED WITH RESISTIVITY ANISOTROPY IN GAS BEARING RESERVOIR OF PORT FOUAD MARINE FIELD, MEDITERRANEAN SEA AREA, EGYPT

M.F. Abu-Hashish[(1)] and A. Almoatar[(2)]

(1) Geology Dept., Faculty of Science, Menoufiya University.
(2) Exploration Dept., Belayim Petroleum Company (Petrobel).

تقييم طبقات الحجر الرملى رقيقة السمك عن طريق تكامل معطيات تسجيلات الرنين النووى المغناطيسى ولاتجانسية المقاومة الكهربية فى خزان وقار البترولى بحقل بور فؤاد البحرى، منطقة البحر الأبيض المتوسط فى مصر

الخلاصة: يقدم هذا البحث أسلوبا تكامليا لتحديد وتقييم طبقات الحجر الرملى رقيقة السمك فى تكوين وقار (من عصر الميوسين) فى حقل بور فؤاد البحرى بمصر، وذلك بسبب تجاوز وعدم قدرة تسجيلات الآبار التقليدية فى التعرف على هذه الطبقات والتى تعتبر قيمة مضافة للمخزون البترولى هناك. ويعتمد الأسلوب المستخدم فى هذا الغرض على تكامل معطيات الرنين النووى المغناطيسى والمقاومة الكهربية اللاتجانسية، حيث أظهرت النتائج فاعلية هذا الأسلوب فى الكشف عن المزيد من الطبقات رفيعة السمك وإمكانياتها البترولية، وتحديد مساميتها ونفاذيتها ومحتواها الهيدروكربونى وإظهار مدى تجانسية الصخر الحامل للمواد الهيدروكربونية وبالتالى إدراك السمك الفعال للخزان البترولى بالمنطقة التى تناولتها الدراسة.

ABSTRACT: *In well logging, delineation of thin beds that contain reasonable amounts of hydrocarbon will enhance the total hydrocarbon potentiality of the area under evaluation. Most of thin beds are usually bypassed in case of the conventional wireline logging tools used, because of their low vertical resolution.*
For better evaluation of the thinly bedded laminated sections and in order to maximize the hydrocarbon potentiality an integrated technique of resistivity anisotropy and nuclear magnetic resonance (NMR) were applied in this study. This approach is very useful, that minimizes the effect of the hydrogen index in the gas bearing sands.
The present study is applied on Port Fouad Marine field, Mediterranean Sea, Egypt, using the data available in the deep well PFMD-1 over the interval 2845-3300 m in the Tortonian Wakar Formation .The results of interpretation show a better definition and counting of the thin beds from 12 m (by conventional tools) compared to 19 m from the NMR-Resistivity anisotropy approach which can be considered as an added value to the formation evaluation process.

INTRODUCTION

Usually, the subsurface reservoir rocks are not homogeneous in their petrophysical characterization. They may contain thin beds that were bypassed by the conventional logging tools, in response of the relatively low resolution of these tools in unraveling the hidden layers.

To tackle this problem, a formation evaluation program was first applied using sophisticated computer software, where the conventional Gamma Ray, Resistivity, Density and Neutron logs are included. This was followed by reevaluation technique in order to establish in more detail the petrophysical characteristics of the formation under study (Wakar Reservoir) using the nuclear magnetic resonance (NMR) data integrated with the resistivity anisotropy results.

The present paper deals with the evaluation of the hydrocarbon potential of the Tortonian Miocene Wakar Formation in Port Fouad Marine field, which is located in the offshore concession to north of Port Fouad City by 36.45 km from the shore line (Egyptian Coast), covering a total area of 144 km². The study area lies between the latitudes 31°43” 58’.40 and 31° 24” 59’.25 N and longitude 32° 18” 01’.72 and 32° 36” 57’.37 E. The water depth is about 26 meters (Fig.1).

Wakar Formation:

Stratigraphically, Wakar Formation (mainly shale and sandstone) is assigned in the Eastern sub-basin to Late Miocene age (Tortonian). It is equivalent to the Qawasim Formation in the central sub-basin and un-conformably overlies the Sidi Salim Formation and underlies the Rosetta evaporates (Kamel et al., 1998) (Fig. 2).

The depth of the Wakar Formation in Port Fouad Marine Field varies from 2540m in the SW of the study area to 2725m at the north. The maximum reached thickness of Wakar Formation in the study area is 763m at the PFM SE-1 well (Fig. 2-6). The gross sand thickness of SI level in Wakar Formation attains the maximum value of 17m at the PFM-1 well. The upper levels of the Late Miocene Wakar Formation were deposited as Highstand Systems Tract (HST) when the late Tortonian sea started to retreat northward due to a marked sea level drop (Barber, 1981).

The late Miocene sand of Wakar Formation was turbidity deposits development of repeated episods of channel-levee, the turbidity period ended up by the development of repeated episodes of channel-levee turbidite type deposits, (Main gas sand reservoirs in Port

Fouad Marine Field). Four channel complexes called SO to S3 have been encountered in the studied wells. The extension of main reservoir "level (S-l)" covers an area more than 25 km^2 (EGPC, 1994).

Nile Delta Tectonic Setting:

The tectonic setting of the Nile Delta region is divided, by the flexure zone that known as hinge line, into two structural sedimentary sub-provinces, the South Nile Delta block and the North Nile Delta basin (Kamel et al., 1998). South of the Flexure, symmetric folds referred to as the Syrian Arc Fold System extend along an actuate trend from the northern Sinai and north of the Gulf of Suez across the southern part of the Delta into the Western Desert (Schlumberger, 1984). The Hinge line has played a dominant role in all the stratigraphic and tectonic evolution of the Nile Delta (Said, 1981, Herms and Wary, 1990). Fig.3 shows that Nile Delta main structural pattern (ENI, 1999).

Structural pattern of the Nile Delta is a complex interplay among main fault trends:

- NW-SE fault trend called Bardawil (Temsah) fault trend.
- NE-SW fault trend called Qattara-Eratosthenes (Rosetta) fault trend, parallel to the Pelusium Lineament (fig. 3).

The Temsah and Rosetta oblique-slip faults intersect in the southern part of deepwater block, creating a faulted, regional high. West of this high, the platform area form an extension of the relatively unstructured Nile delta province to the south (Barsoum et al., 1998, Abdel Aal et al, 2000).

The Northern Delta basin is characterized by two main structure patterns as follows:

1. **Deep pre-Tortonian fault pattern** (possibly to Eocene-or Late Cretaceous) mainly of E-W fault blocks, prominent among which are the Shelf margin structures, which play a great role on the Miocene subsidence and sedimentation.

2. **Shallow post-Messinian fault pattern**, which is genetically related to the sedimentary load of the recent sediments at the unstable Delta margin, this caused growth faulting, slumping and normal faults as well as diapirism of un compacted Pliocene and Messinian evaporites (Kamel et al., 1998).

Both sets of structures, however, appear to have been modified and governed by NW-SE and NE-SW trending faults. The old fault systems which were rejuvenated in Late Oligocene and younger ages controlled the distribution of the Miocene and younger sequences.

The basins yielded great facies and thickness variations, which also were controlled by the tectonic events. These later faults formed three major tectonic-sedimentary sub-basins, which are called Eastern, Central and Western sub-basins (Fig. 4).

1. Eastern Sub-Basin:

The NW-SE trending Temsah faults separates the Eastern sub-basin from the Central sub-basin. In this basin the Wakar Formation un-conformably overlies the Sidi Salem Formation and underlies the Rosetta evaporates (Kamel et al., 1998).

2. Central Sub-Basin:

It is separated from the Eastern and Western sub-basins by set of fault trending NW-SE and NE-SW direction, namely, the Temsah and Rosetta faults, respectively (Kamel et al, 1998).

The Late Miocene (Messinian stages) Qawasim and Abu Madi Formations (shales and sandstones) overlie unconformably the Sidi Salem Formation.

3. Western Sub-Basin:

The NE-SW trending Rosetta faults define and separate the Western sub-basin from the Central basin (Kamel et al., 1998).

Thin Beds:

Saxena et al. 2006, define thin bed as: all the geological beds and laminae less than two feet. In our study we consider the thin bed as whose thickness below the vertical resolution of the conventional logging tools. Every tool has its definition of thin bed thickness according to its sensitivity to delineate it.

NMR Physics:

NMR logging works by forcing the hydrogen nuclei of the formation fluids into a spin, and then monitoring the rate and the way in which they recover stability (Cannon, et al., 1998, Xiao, et al., 2012).

The Combinable Magnetic Resonance (CMR) tool is a pad-type tool that performs pulsed NMR measurements using Carr - Purcell - Meiboom - Gill (CPMG) pulse sequences. The spin – echo signals acquired during the measurement are derived from protons (i.e. hydrogen nuclei) that process in the static magnetic field by a permanent magnet in the tool antenna (Nashaat, et al., 2001, Noah, et al., 2014).A CPMG consists of two time intervals:

1. An initial wait time (WT) during which the proton magnetization approaches its thermal equilibrium value in the static magnetic field.
2. Echo collection period during which a set of radio frequency (RF) pulses generated by the tool antenna are used to generate the spin echoes.

A cut-off value is established, depending on the lithology, to distinguish between bound fluid and free fluid from the pore size distribution. Typically, a value of 33 msec will be used for sandstone and a value of 100 msec will be used for carbonates. (Fig. 5 shows the T2 distribution with the cut-off used).

CMR applications:

Recently, it was shown how to combine the NMR with the Density measurement to estimate the gas corrected total porosity. The technique is called Density Magnetic Resonance (DMR). The main inputs to the DMR technique are the Density and the CMR total porosity (Nashaat, et al., 2001).

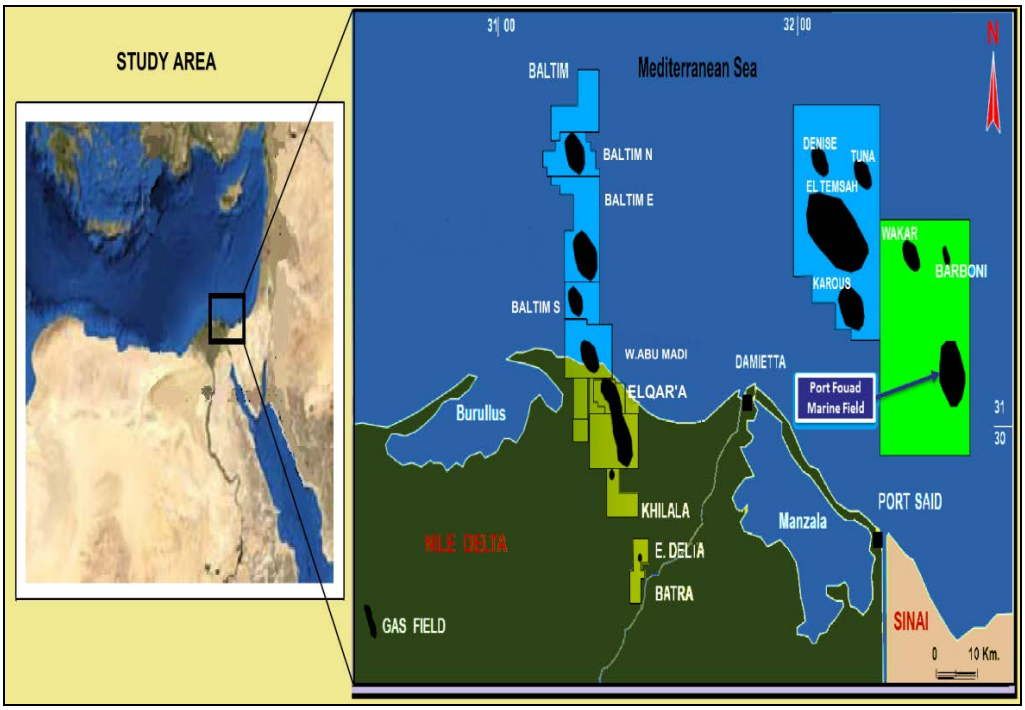

Fig. (1): Location map of the Port Fouad Marine gas Field.

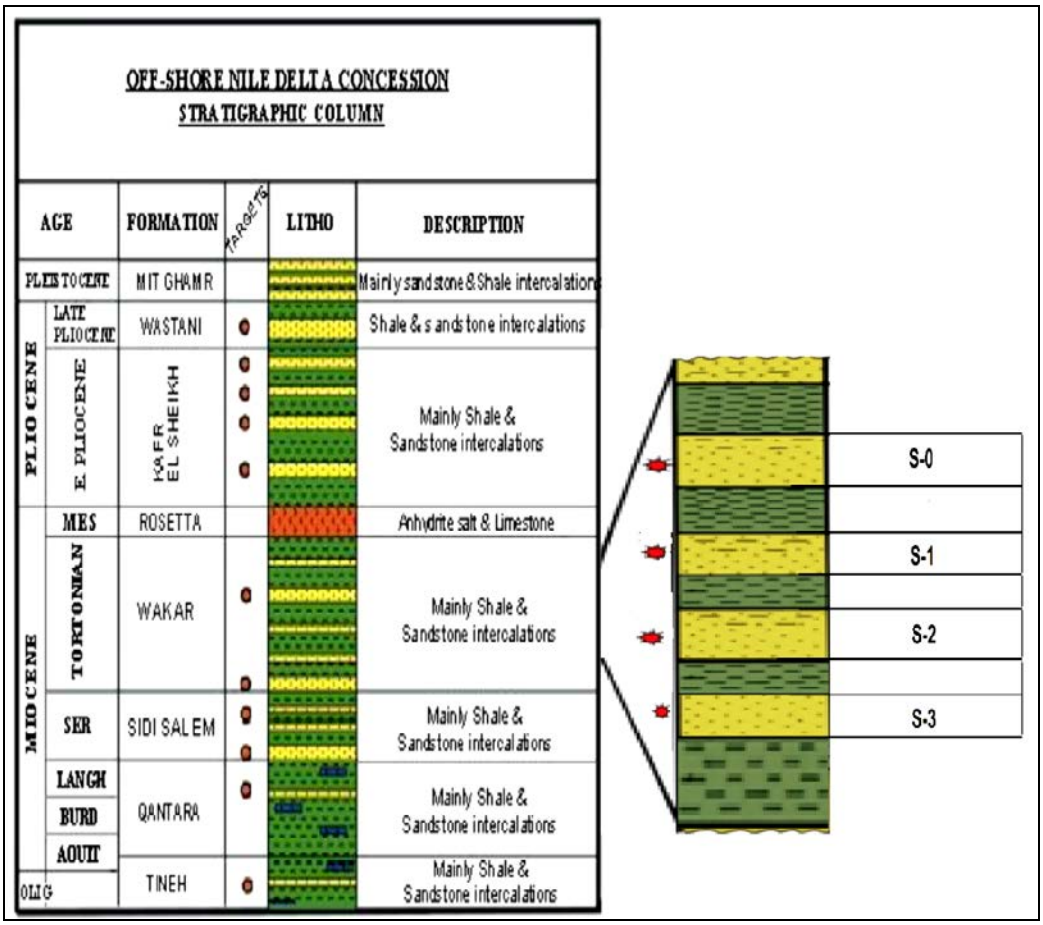

Fig. (2): Generalized Stratigraphic Column of the Offshore North-Eastern Part of Nile Delta (after Kamel, et al., 1998, Badri, et al., 2000, ENI, 2008).

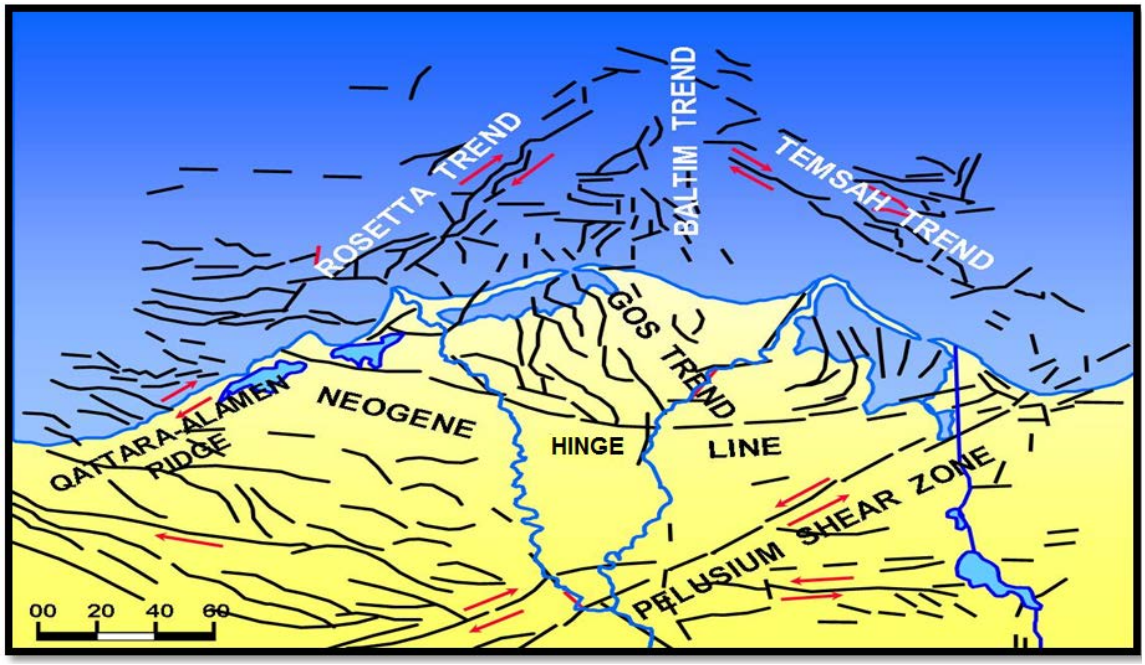

Fig. (3): The Nile Delta main structural pattern (Eni, 1999).

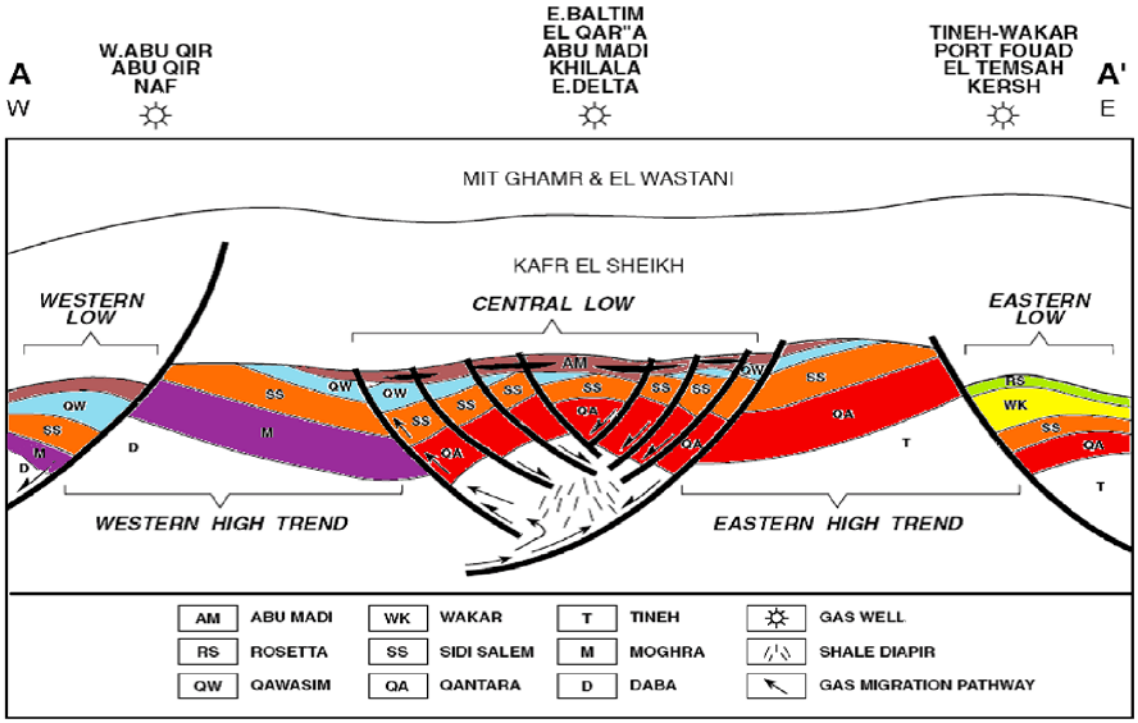

Fig. (4): Geologic model of north delta block (Kamel et al., 1998).

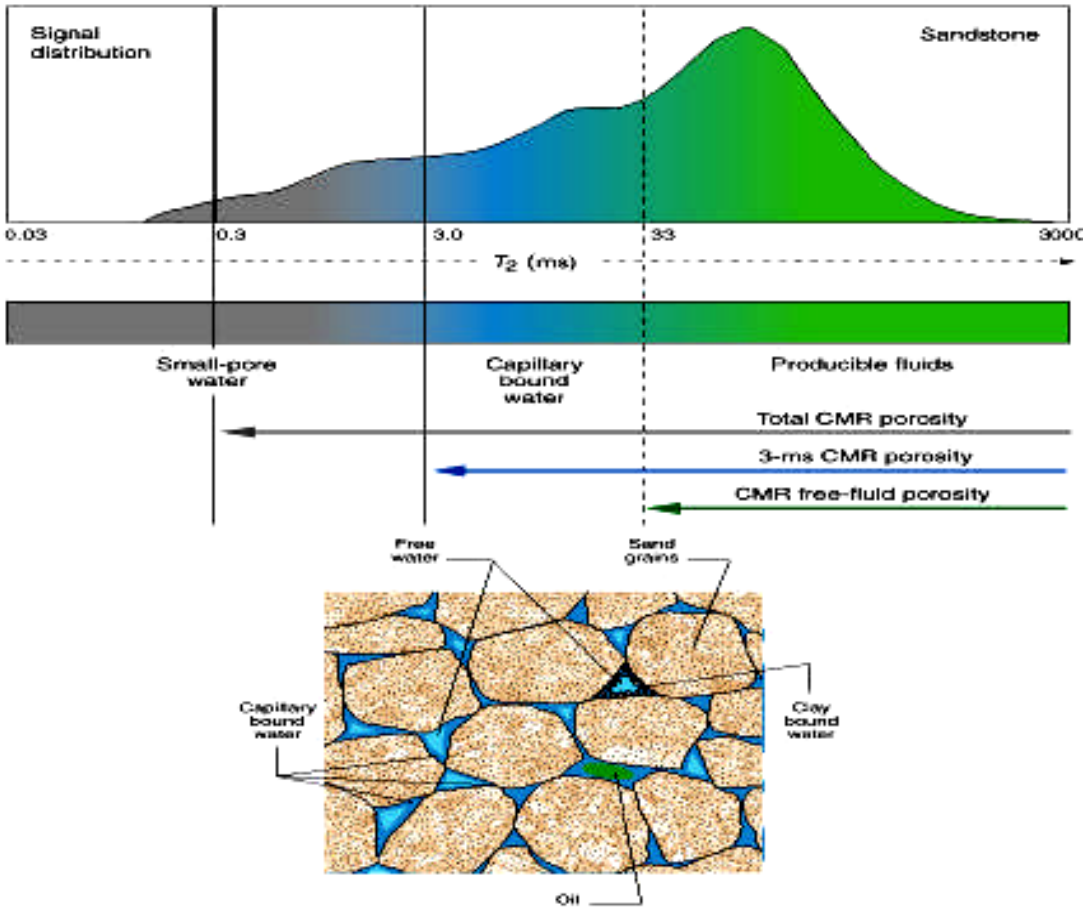

Fig. (5): Pore size distribution from the CMR, (after Coates, et al., 2000).

The resulting outputs are:

a) Gas Corrected Porosity.

b) Gas Saturation in the invaded zone.

c) Gas Corrected Permeability.

a) NMR porosity:

The fact that NMR porosity depends only on the fluids content of the formation, unlike density and neutron porosity, which is influenced by both fluids and surrounding rocks, makes NMR measurements much more capable than conventional logs to furnish clay corrected, nonproductive and productive porosities. In zones containing light hydrocarbon, where the hydrogen index is less than unity, NMR porosity will typically underestimate true porosity in proportion to the hydrogen index (Dunn, et al., 2002).

The initial amplitude of the raw decay curve is directly proportional to the number of Polarized hydrogen nuclei in the pore fluid. The raw reported porosity is provided by the ratio of this amplitude to the tool response in a water tank (which is a medium with 100% Porosity). This porosity is independent of the lithology of the rock matrix and can be validated by comparing laboratory NMR measurements on cores with conventional laboratory porosity measurements.

The accuracy of the raw reported porosity depends primarily on three factors:

- A sufficiently long TW to achieve complete polarization of the hydrogen nuclei in the fluids.
- A sufficiently short TE to record the decays for fluids associated with clay Pores and other pores of similar size.
- The number of hydrogen nuclei in the fluid being equal to the number in an equivalent volume of water, that is, HI = 1(Coates, et al., 2000).

(a) Porosity Estimation in Gas-bearing Formation:

the method of calculating Porosity from NMR Log is based on the following equation as follows (Xiao, et al., 1998, 2012):

$$CMRP = \phi * Sg * HIg + \phi * HIf\ (1-Sg)$$

$$= \phi\ \{Sg * HIg * Pg + HIf\ (1-Sg)\} \qquad (1)$$

where: $Pg = 1-\exp\{-(Tw/Ti,g)\}$

CMRP: NMR porosity that can be acquired from the NMR log directly

ϕ : formation porosity (in %).

Sg : gas saturation in fraction.

HIg : hydrogen index of natural gas.

Hlf : hydrogen index of pore fluid (in fractions).

Pg : polarization factor.

Tw : polarization time.

Ti,g : longitudinal relaxation time of natural gas (in microseconds).

For fully water-saturated rocks, HIf is taken to be 1.0 and Equation (1) can be rewritten as follows (Xiao, 1998, Coates, et al., 2000):

$$CMRP/\phi = I\text{-}Sg\ (l\text{-}Ig*Pg) \quad (2)$$

Then porosity must be calculated first to obtain information about Sg.

(b) NMR Enhanced Water Saturation with Resistivity Data:

Because resistivity tools have a large depth of investigation, a resistivity-based water saturation Model is preferred for determining water saturation in the virgin zone of a formation. However, resistivity measurements cannot distinguish between capillary-bound water and movable water. This lack of contrast makes it difficult to recognize hydrocarbon productive low-resistivity and/or low-contrast pay zones from data provided by traditional logging suites.

The unique information, such as bulk volume of irreducible water (BVI) and clay-bound water (CBW), provided by NMR logging can significantly enhance the estimation of resistivity-based water saturation and can greatly assist in the recognition of zones that will produce water-free.

NMR data and the deep resistivity data are integrated to determine whether producible water is in the virgin zone, or whether an interval with high water saturation may actually produce water-free hydrocarbons (Coates, Xiao, Primmer, 2000).

(c) NMR permeability:

NMR relaxation properties of rock samples are dependent on porosity, pore size, pore-fluid Properties and mineralogy. The NMR estimate of permeability is based on theoretical models that show that permeability increases with both increasing porosity and increasing pore Size.

The permeability can be derived from the above measurement using one of the following two methods (Timur. 1969, Nashaat,. et al., 2001):

(1) Timur - Coates empirical equation:

$$K = A*(CMFF/BFV)^2*(TCMR)^4 \quad (3)$$

in which:

K = Permeability (in mD)

A = Constant (Calibration Factor).

CMFF = NMR porosity above the T2 cut-off.

BFV = NMR porosity below the T2 cut-off.

TCMR = NMR total porosity.

2) SDR equation:

$$K = C*(T2lm)^2*(TCMR)^4 \quad (4)$$

in which:

K = Permeability (in mD).

C = Constant (Calibration Factor).

T2lm = Logarithmic mean of the T2 distribution.

TCMR = NMR total porosity.

The main advantage of the SDR technique is the simplicity and the fact that there is no need for a T2 cutoff estimation. The main limitation of the SDR technique is that it cannot be used in gas bearing formations or when oil base mud is used (Nashaat, et al., 2001).

For the above-mentioned reasons, only Timur / Coates permeability equation was used throughout this paper.

Formation Anisotropy: Reckoning with its effects:

Anisotropy, the opposite of isotropy, is widely known in the oil patch, Anisotropy as applied to reservoir rock describes the well-known fact that properties such as fluid current flow and acoustic propagation may vary dramatically with direction. Anisotropy is virtually assured by the sedimentary process and subsequent tectonic stress, formations deposited in flow, electric horizontal beds are almost certain in behaving differently horizontally than vertically. A rock (that is fractured vertically will behave differently depending on horizontal direction.

Resistivity anisotropy technique is important for thin bed evaluation which depends on the difference between vertical resistivity (R_v) and horizontal resistivity ($R_н$). If $R_v = R_н$, that means isotropic rock (may be no thin lamina), If $R_v \neq R_н$ that means anisotropic rock (may be of thin lamina). Anisotropy can be calculated from the ratio of R_v over $R_н$.

Resistivity anisotropy concept:

As early as 1920, Conrad Schlumberger recognized that anisotropy affected the formation's DC electrical properties that he rind begun measuring using electrode array strung along the earth's surface (Schlumberger C1920, Schlumberger, Leonardon, 1934).In 1932, Schlumberger pioneers Maillet and Doll reported investigations into electrical conduction for a particular class of anisotropic media, confusingly called transversely isotropic (Maillet, Doll, 1932). A transversely isotropic formation has the same resistivity in any horizontal direction, but a different resistivity in the vertical direction.

Transversely isotropic medium could be made electrically isotropic by simply rescaling the anisotropic axis by a factor λ, the anisotropy coefficient:

$$\lambda^2 = R_v/R_н \quad (5)$$

In which R_v and $R_н$ are vertical and horizontal resistivity.

In anisotropic media, the three main logging methods to determine electrical resistivity namely unfocused current, induction logging and laterologging

all basically respond to the horizontal electrical properties of the formation as shown in fig. (6).

The ratio between the resistivity value in the vertical direction R_v, and that in horizontal direction $R_н$ to know as anisotropy coefficient, λ.

(i) Anisotropy in sands:

Water saturated sandstones have an intrinsically low electrical anisotropy ratio. Laboratory measurements of wet sandstone samples have shown that their anisotropy ratios are generally less than 1.6. In situ measurements of water sands have confirmed the laboratory findings. Certain types of hydrocarbon bearing sandstones that are at irreducible water saturation have been proven to have high anisotropy ratios. There are two generally accepted models of such formations. Sandstones can also exhibit a relatively high electrical anisotropy without hydrocarbons being present.

Layers of low porosity, tightly cemented sand interbedded with more porous sand layers, can create an anisotropy ratio that may be higher than characteristic of water sand. Fig. 6 shows the effect of changes in sand/shale volume and oil saturation on the resistivity anisotropy. It can be seen that for this case, where we have 50% shale, a change in saturation will have little effect on the parallel (horizontal) resistivity, $R_н$, while the effect on the perpendicular (vertical) resistivity, R_v is much more noticeable.

(ii) Anisotropy in Shales:

Electrical anisotropy ratios in shale have been measured up to 7.3, although generally are between 1 and 4. Compaction and dewatering of mud gives rise to the source of electrical anisotropy in shale. These processes typically create a preferential axis of orientation of clay platelets within the shale. The mobility of clay counter ions near the surface of these platelets provides an increased conductivity in their plane of orientation. Fig. 8 shows Photomicrograph of shale clay platelets distributed around the horizontal.

Inversion for Resistivity Anisotropy:

The formation resistivity anisotropy is characterized by acquiring a combination of induction and laterolog. It is known that the measurement of an induction tool is limited to the plane perpendicular to the tool, while the measurement for a laterolog tool is effected by both horizontal and vertical resistivity. In lateral logging, anisotropic layer of thickness $h_{LAT}$is equal to the product of the coefficient of anisotropy and true thickness, while the resistivity ϱ_{LAT} is equal to the geometrical mean resistivity (Keller, et al., 1966):

$$h_{LAT} = \lambda * h \qquad (6)$$

$$\rho_{LAT} = \lambda * \rho_н = \sqrt{(\rho_v * \rho_н)} = \rho_m \qquad (7)$$

Where ϱv and ϱh are the vertical and horizontal resistivities, respectively. The coefficient of anisotropy λ is defined by $\sqrt{\left(\frac{ev}{eh}\right)}$ where h is the true thickness. From equation (3 & 4), the coefficient of anisotropy λ and the true thickness h can be defined.

Induction logging gives only the horizontal resistivity of a layer, while the thickness is undistorted, so that:

$$h(ind) = h \qquad (8)$$

$$\varrho^{(ind)} = \varrho h \qquad (9)$$

From the equation (5) and (6) we can get the true thickness h and the horizontal resistivity ϱh of a layer directly by neglecting the effects on borehole, shoulder and invasion. We still cannot determine the coefficient of anisotropy and hence cannot resolve the full resistivity information only by induction or lateral logging separately.

We can first resolve the true thickness h and horizontal resistivity ϱh by induction log. Then substituting h and ϱh into equation (4), we will be able to resolve the coefficient of anisotropy λ. Thus we can get the horizontal resistivity, the coefficient of anisotropy, and the thickness of each layer by joint inversion of induction and lateral logs (Wei, Yang, 2003).

Case Study:

As mentioned earlier, this paper deals with the evaluation of hydrocarbon potentialities of the Tortonian Miocene Wakar Formation in Port Fouad Marine field. This formation consists of Sandstone intercalation with Shale that contain thinly bedded of Sandstone. Data from the deep PFMD-1 well constitute the main source used in this study.

Data Availability and Quality Control:

The logging program, over the section of interest, was devised to maximize the quality of the information available in the thinly bedded zones. In addition to conventional TLD density, APS neutron porosity and AIT induction resistivity, the OBMI (oil base mud micro imager) provided a resistivity anisotropy measurement to evaluate both the horizontal and vertical formation resistivities.

The CMR log, corrected for gas effect using the density porosity assuming a formation matrix density of 2.67 g/cc, provided the total porosity, clay-bound and capillary-bound water, and free fluid index. An estimation of the formation permeability, using the gas corrected CMR-derived total porosity was also obtained. Due to the general physics of the measurement, all induction tools have a range of validity that is limited to a maximum ratio of formation to mud resistivity (Fig. 9).

All logs were depth matched to the wire line open-hole resistivity log. No additional editing of raw data was required. The HNGS (Hostile Environment Gamma Ray Sonde) log was corrected for potassium and barite effects. The methodology and interpretation work flow is illustrated in Fig. 10.

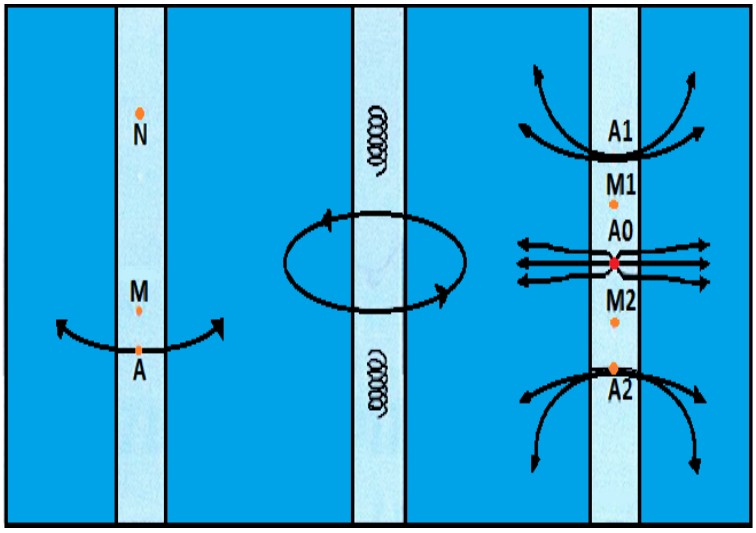

Fig. (6): Maillet and Doll's simple model. (after Schlumberger, Oilfield Review, Jan., 1990).

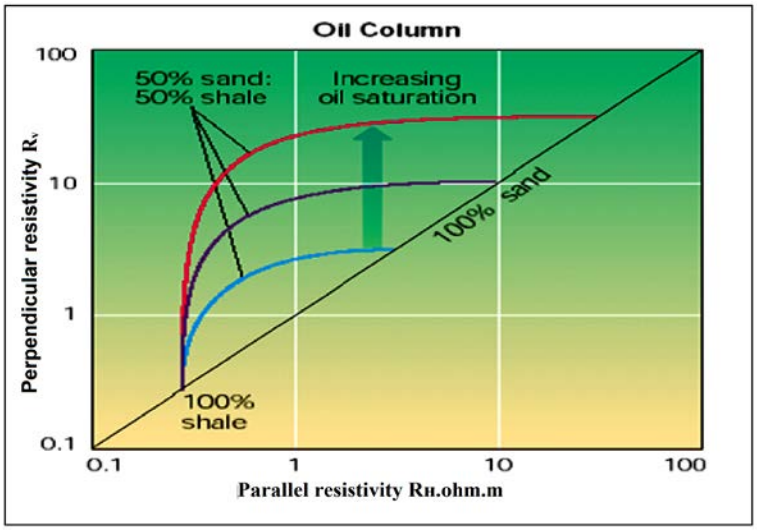

Fig. (7): The effect of changes in sand/shale volume and oil saturation on the resistivity anisotropy. (after Petrobel Company, 2004).

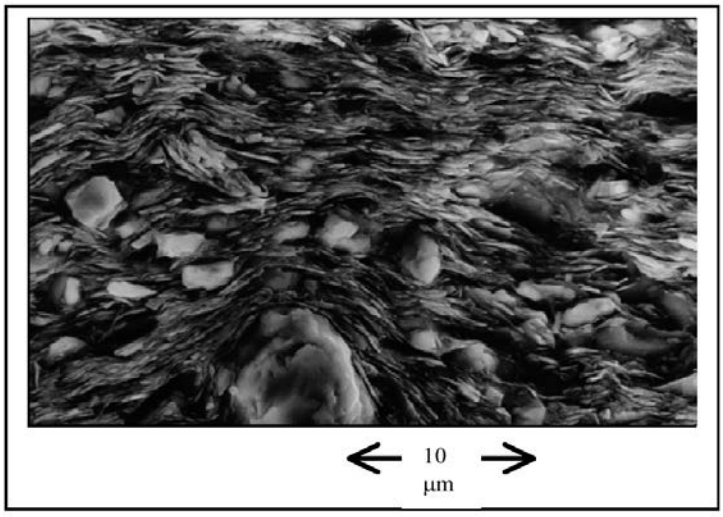

Fig. (8): Photomicrograph of shale. (After Petrobel Company, 2004).

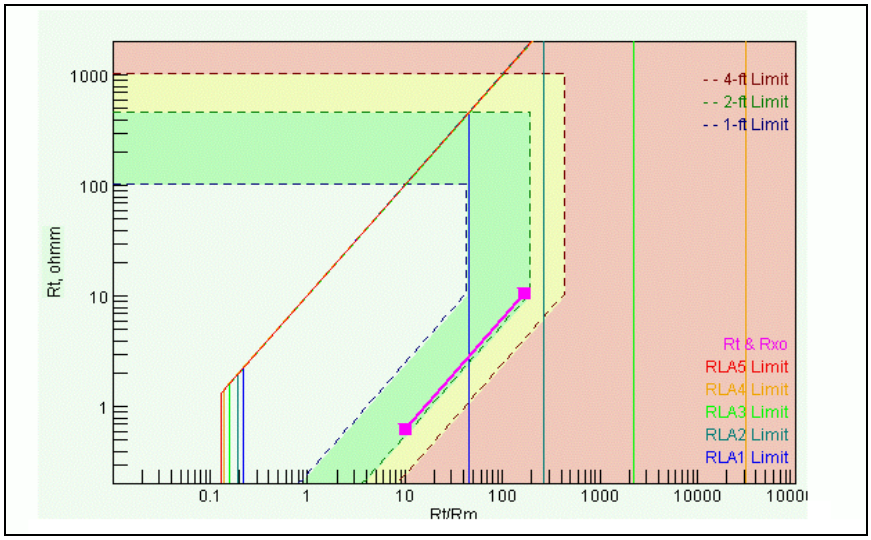

Fig. (9): Range of measurement for resistivity tools. (Courtesy of Petrobel Co.2004).

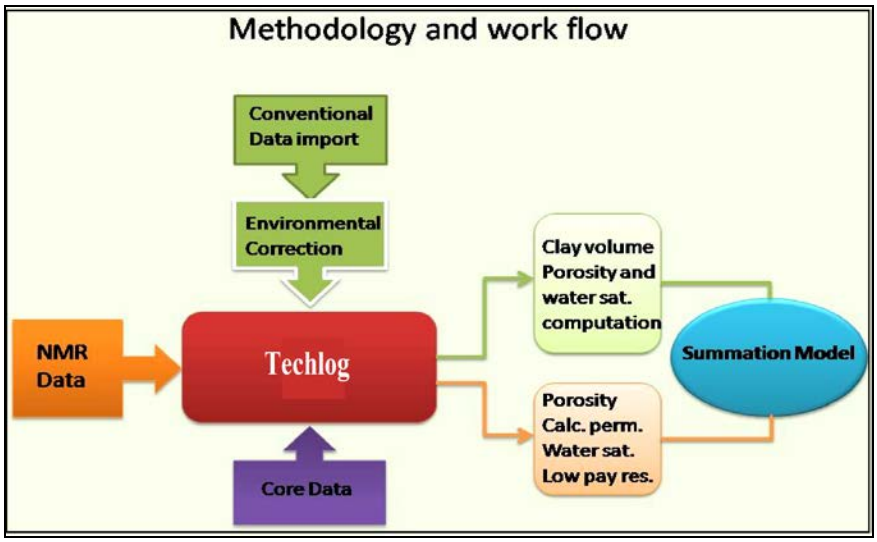

Fig. (10): Methodology and interpretation work flow.

Table (1): Average petrophysical parameters of Wakar Formation

A) From conventional Logging tools

Formation	Zone	Top	Bottom	Thickness	Net Pay	Porosity	S_W	V_{SH}
		m	m	m	m	%	%	%
WAKAR Fm	S-0	2968	3011	43	4.5	28	45	12
	S-1	3076	3129	53	7.5	24	48	14

B) From NMR tool:

Formation	Zone	Top	Bottom	Thickness	Net Pay	Porosity	S_W
		m	m	m	m	%	%
WAKAR Fm	S-0	2968	3011	43	6	26	35
	S-1	3076	3129	53	13	25	50

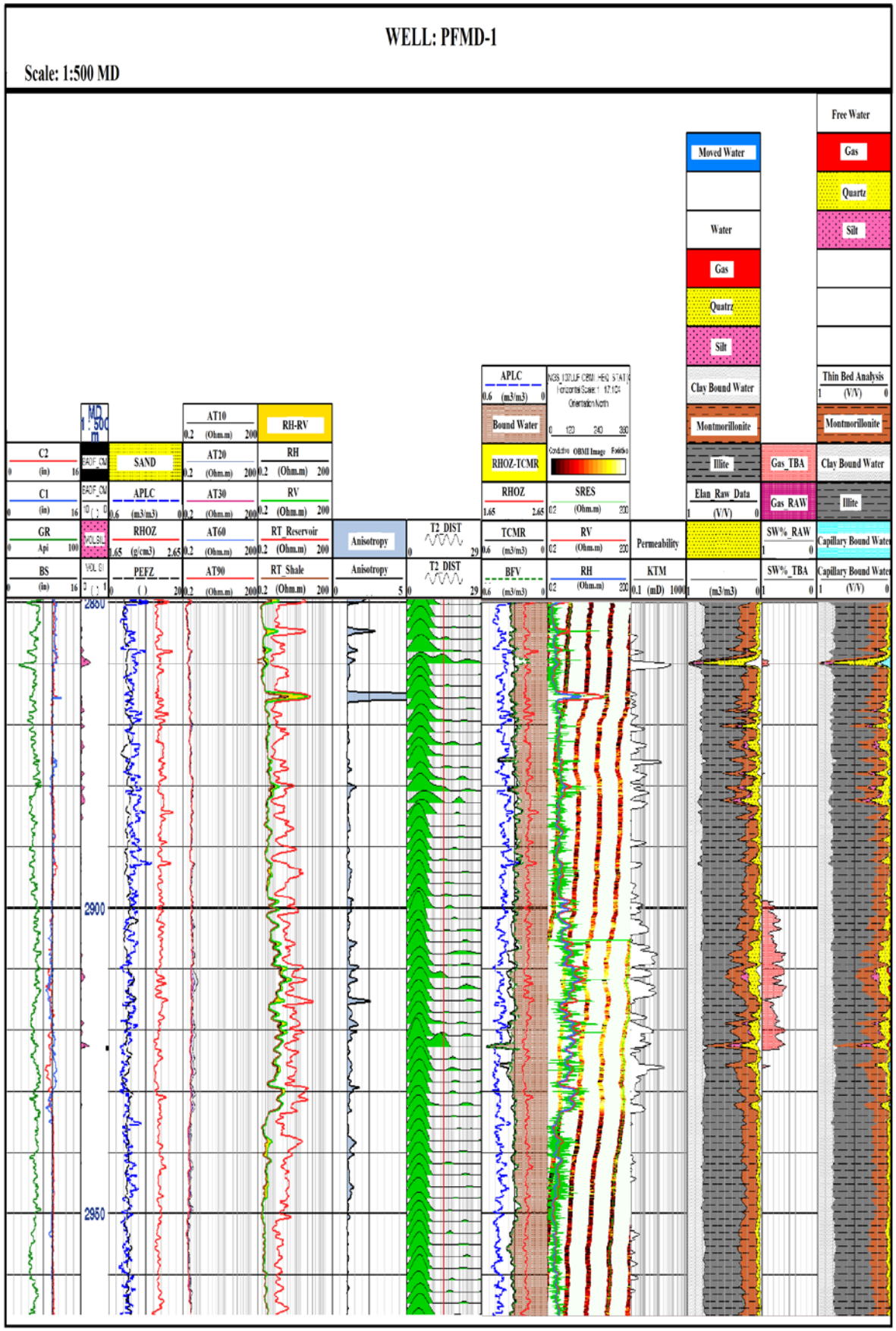

Fig. (11): Resistivity Anisotropy and Thin Bed Analysis from 2900 to 2925 m due to with average Sw = 65% .Confirmed by KTIM permeability from CMR.

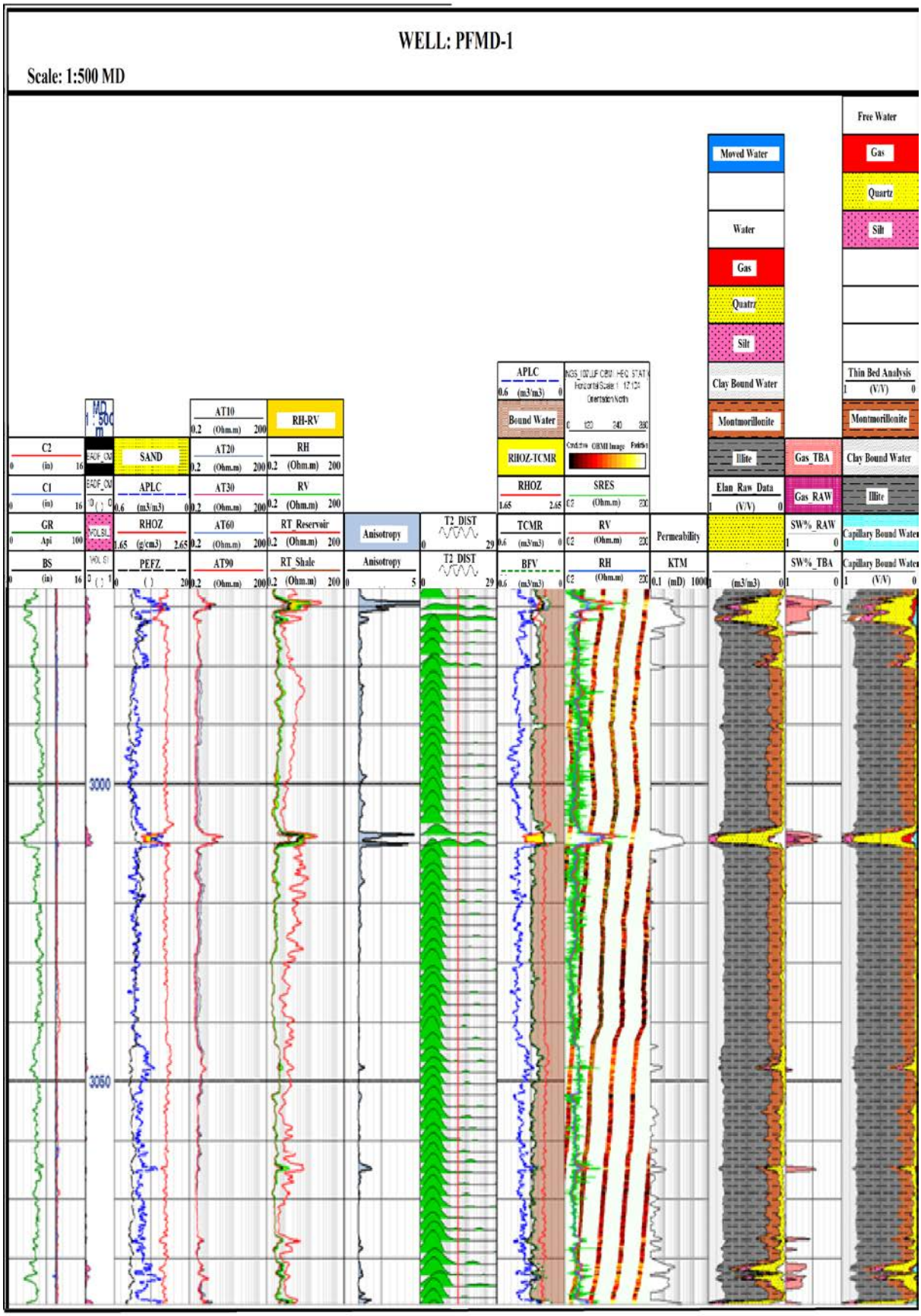

Fig. (12): Resistivity Anisotropy and Thin Bed Analysis from 2969 to 2972.5 m with average Sw = 35%. Confirmed by KTIM permeability from CMR.

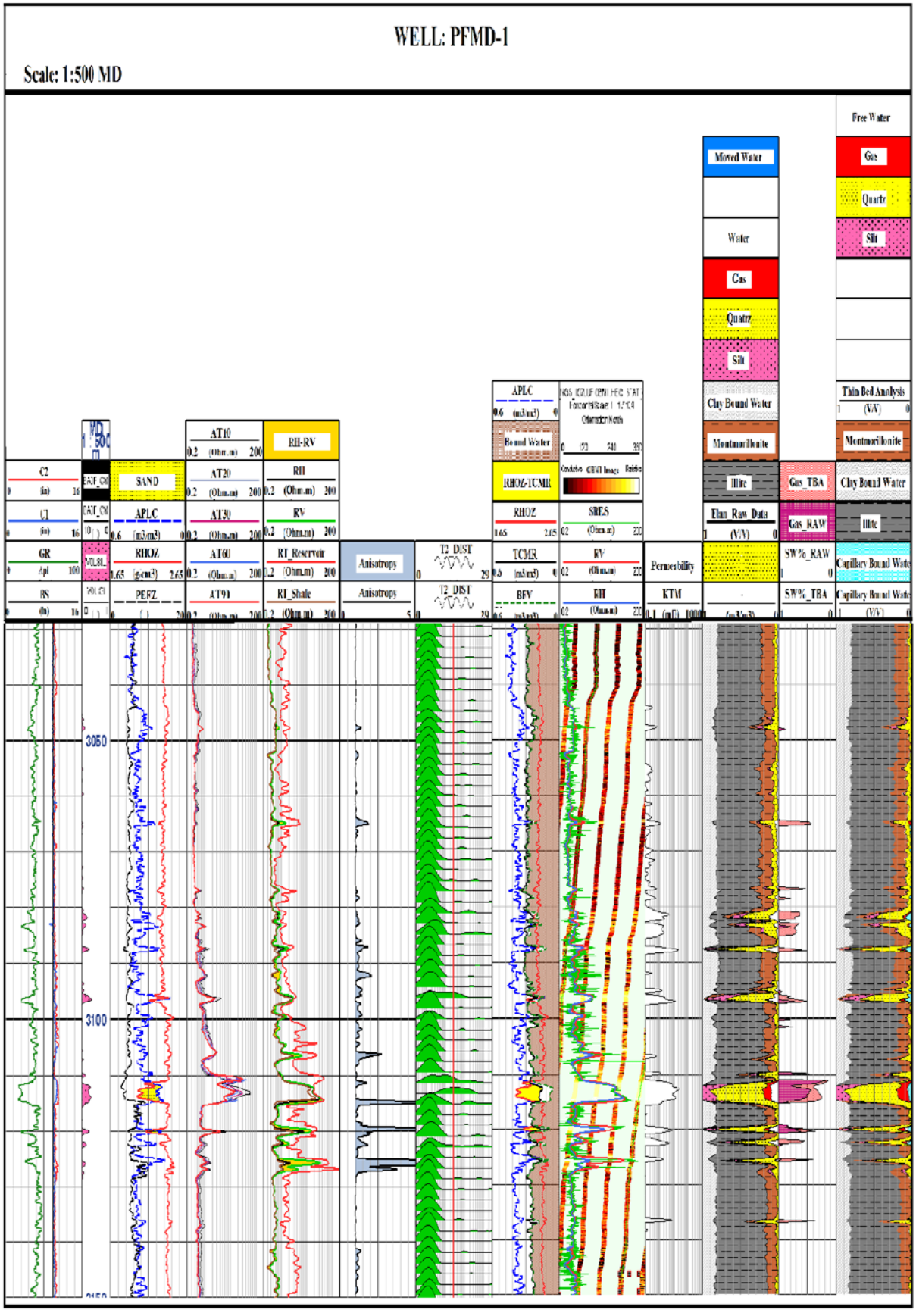

Fig. (13): Resistivity Anisotropy and Thin Bed Analysis from 3064 to 3065 m and from 3080-3127 m with average S_w = 50%. Confirmed by KTIM permeability from CMR.

DISCUSSION

The results from CMR and resistivity anisotropy over the main reservoir sand Wakar Formation, where we can see that the anisotropy technique indicates higher anisotropy in some intervals supported by CMR results. The results show a clear anisotropy from 2900 m to 3127 m due to the thinly bedded laminated sand-shale gas with average Sw = (35%-65%). This was confirmed by the KTIM permeability from CMR but there is no anisotropy opposite the gas bearing massive sand from 3111 to 3115 m. The petrophysical parameters of Wakar Formation derived from both conventional logging tools and NMR are summarized in table 1.

CONCLUSIONS

- The use of advanced technology in the open hole logging in combination with conventional logging tool is mandatory for proper evaluation in the Mediterranean gas bearing sandstone, especially in the low resistivity thin beds.
- Nuclear Magnetic Resonance (NMR) has emerged as a leading technological break-through, which is providing difficult-to-interpret zones with the outstanding results. Unlike other conventional tools, the NMR measurements are largely based on the fluid and the pore space characteristics. This makes it possible to see the fluids and pores more obviously which are not seen on other conventional logs like Density, Neutron, Sonic and Resistivity.
- The combination of NMR wireline tools with Resistivity Anisotropy show how the resistivity data are useful for thin beds detection depending on rock homogeneity. The difference between vertical and horizontal resistivity gives a good idea about the rock homogeneity. Therefore, we can identify and quantify resistivity anisotropy by joint inversion.
- As regards the Wakar Formation in Port Fouad Marine field, the integrated approach using conventional logging tools and advanced tools has shown very helpful in studying the reservoir parameters in this field, particularly in the detection of thinly bedded zones that are usually bypassed by conventional logging tools of limited resolution, thus hiding additional hydrocarbon reservoirs.
- Log analysis in well PFMD-1has shown an increase from 12 m to 19 m in the reservoir effective knowledge of its petrophysical characteristics, namely porosity, permeability, gas saturation, lithology and heterogeneity. This knowledge can serve in choosing the RFT or MDT points for reservoir pressure measurements and delineation of fluid contacts. A good idea about reservoir permeability can increase the chance for carrying out frac jobs if required.

ACKNOWLEDGEMENT

The authors wish to express their thanks and gratitude to the EGPC (The Egyptian General petroleum Corporation) and PETROBEL (Belayim Petroleum Company) for releasing data used in this work.

REFERENCES

Abdel Aal, A., EI-Barkooky, A., Gerrits, M., Meyer, H., Schwander, M. and Zaki, H., 2000. Tectonic evolution of the eastern Mediterranean basin and its significance for hydrocarbon prospectivity in the ultra-deepwater of the Nile Delta, The leading edge, October 2000, PP.1086-1102.

Barsoum, K., Aiolfi, C, Dalla, S., Kamal, M., 1998. Evaluation and Hydrocarbon occurrence in the Plio-Pleistocene succession of the Egyptian Mediterranean margin: Examples from the Nile Delta basin, Proceedings of 14th petroleum conference, Cairo, October, 1998, EGPC, Vol.1, pp. 386-401.

Archie, G.E, 1942. The electrical resistivity log as an aid in determining some reservoir characteristics, Petroleum Transactions of the AIME 146 pp:54-62.

Chemali, R, Gianzero S, susm, 1987. The Effect of shale anisotropy on focused resistivity devices, transactions of the SPWLA 28th annual logging symposium, London, England.

Cannon, E.D., et al. 1998. Quantitative NMR interpretation SPE 49010, SPE Fall Meeting, New- Orleans, USA.

Coates, G.R., Xiao, L.Z., Primmer, M.G., 2000. NMR Logging Principles and Applications, Gulf Publishing Company, Houston, USA, pp: 1-200.

Dunn, K.J., Bergman, D.J., Latorraca, G.A., 2002. Nuclear Magnetic Resonance: Petrophysical and Logging Applications, Handbook of Geophysical Exploration, Pergamon, New York, pp: 1-120.

EGAS (Egyptian Gas Holding Company) annual report released in January 2012.

EGPC (Egyptian General Petroleum Corporation), 1994. Nile Delta and North Sinai: a Field, Discoveries and hydrocarbon potentials (A comprehensive overview), Egyptian General Petroleum Corporation, Cairo, Egypt, 387p,

Kunz, K.S., Moran, J.H., (1958). Some Effects of Formation Anisotropy on Resistivity Measurements in Boreholes, Geophysics 23,pp: 770-794.

Kamel, H., Eita, T. and Sarhan, M., 1998. Nile Delta hydrocarbon potentiality: EGPC, 14th Petrol. Exp. Prod. Conf., Cairo, vol. 2, p. 485 -503.

Keller, G.V., Frischknecht, FG, 1966. Electrical Method in Geophysical prospecting, Pergamon Press. inc.

Kenyon, W.E., 1997. Petrophysical principles of applications of NMR logging. Log. Anal.,38(3): 21-43.

Maillet, R, Doll, H.G, 1932. Sur UN théorème relatif aux milieux électriquement anisotropes et ses applications à la prospection électrique en courant continu, erganzungshefte fur angewandtegeophysik 3 (theory of electrically anisotropic media and its applications to electrical prospecting). pp:109-124.

Moran, J. H. Gianzero, S., 1979. Effects of formation anisotropy on resistivity logging measurements, Geophysics 44 pp: 1266-1286

Nashaat, M., Sallam, Y., Elsherif, A., 2001. Utilizing magnetic resonance logging for improved formation evaluation in the Mediterranean thinly laminated gas bearing formations: A Case Study, Society of Petroleum Engineers.

Noah, A., Shazly, T., 2014. Calculation of porosity by combining the Nuclear Magnetic Resonance and Sonic logs in gas bearing Reservoir at Sienna Field of WDDM Concession in Egypt, World Applied Sciences Journal, pp.: 1801-1807.

Runge, R. J., Hill, D. G. 1971. The role of anisotropy in ULSEL, Transactions of the SPWLA 12th Annual Logging Symposium, Dallas, Texas, USA.

Schlumberger, M. Leonardon, E. G, 1934: Some observations concerning electrical measurements in anisotropic media and their interpretation, Transactions of the American Institute of Mining and Metallurgical Engineers 110 pp: 159-182.

Schlumberger Oilfield Review, Jan., 1990. Formation Anisotropy: Reckoning with its effects, vol.2, issue:1, pp:16-18.

Timur, A., 1969. Pulsed Nuclear Magnetic Resonance studies of porosity, movable fluid and permeability of Sandstone, JPT Journal, Vol. 21, 1969.

Xiao, L. Z., 1998. Magnetic Resonance Imaging Logging and Rock Nuclear Magnetic Resonance and its application, Science Press, Beijing (in Chinese).

Xiao, L., Zhi-qiang, Mao, L., Gao-ren, Yan, Jin, 2012. Calculation of porosity from Nuclear Magnetic Resonance and conventional logs in gas-bearing reservoir. Acta Geophysica, 60: 1030-1042.

Wei, Yang, 2003. Determining Resistivity anisotropy of geological formation by joint inversion of lateral and Induction logs, vol. 25, no. 2, pp: 274-279.